

The Macroscopic Detection of Corrosion  
in Aluminum Aircraft Structures With  
Thermal Neutron Beams and Film  
Imaging Methods

A Report  
Submitted to the U.S. Naval Air  
Systems Command, Washington, DC  
USN Contract No. N00019-76-IP-69007

December 7, 1977

Report Prepared

by

Donald A. Garrett  
Reactor Radiation Division  
Institute for Materials Research  
National Bureau of Standards  
Washington, DC 20234

Work Performed By

William Parker, Ph.D.  
Martin Ganoczy  
Michael Dorsey  
Donald A. Garrett



The Macroscopic Detection of Corrosion  
in Aluminum Aircraft Structures With  
Thermal Neutron Beams and Film  
Imaging Methods

A Report  
Submitted to the U.S. Naval Air  
Systems Command, Washington, DC  
USN Contract No. N00019-76-IP-69007

Report Prepared

by

Donald A. Garrett  
Reactor Radiation Division  
Institute for Materials Research  
National Bureau of Standards  
Washington, DC 20234

Work Performed by

William Parker, Ph.D.  
Martin Ganozcy  
Michael Dorsey  
Donald A. Garrett



## Table of Contents

	<u>Page</u>
Abstract	1
1.0 Objectives	2
2.0 Background	2
3.0 Experimental Facilities at NBS	3
4.0 Experimental Procedures: General	3
5.0 Technical Approach	6
6.0 Exposure Series 1 Through 3: General	6
6.1-A Exposure Series 1A	9
6.1-B Exposure Series 1B	12
6.1-C Exposure Series 1: Results and Conclusions	12
6.2-A Exposure Series 2A	15
6.2-B Exposure Series 2B	16
6.2-C Exposure Series 2: Results and Conclusions	21
6.3-A Exposure Series 3A	21
6.3-B Exposure Series 3B	22
6.3-C Exposure Series 3: Results and Conclusions	25
6.4-A Exposure Series 4	28
6.4-B Exposure Series 4: Results and Conclusions	29
7.0 Quantification of Corrosion	32
8.0 Remarks and Qualifications	32
9.0 Summary	33
10.0 Recommendations for Future Investigations at NBS	34
10.1 Converter Development	34
10.2 Real Time Imaging Methods for Corrosion Detection	35
10.3 Corrosion Quantification - Standard Penetrometer Development	36



## Tables

	<u>Page</u>
Table 1A Exposure Series 1A: Radiographic Parameters	9
Table 1B Exposure Series 1B: Radiographic Parameters	12
Table 2A Exposure Series 2A: Radiographic Parameters	16
Table 2B Exposure Series 2B: Radiographic Parameters	16
Table 3A Exposure Series 3A: Radiographic Parameters	22
Table 3B Exposure Series 3B: Radiographic Parameters	25
Table 4 Exposure Series 4: Radiographic Parameters	28
Table 5 Penetrometer Calibration	29



## Figures

### Page

Fig. 1 Schematic Diagram of the NBS Thermal Neutron Radiography Facility	4
Fig. 2 C-2 Aircraft Vertical Fin Section	5
Fig. 3A Aluminum Corrosion Penetrometer P-1	7
Fig. 3B Aluminum Corrosion Penetrometer P-1 - Close Up View	7
Fig. 4 Aluminum Corrosion Penetrometers P-2-1 through P-2-4	8
Fig. 5 Exposure Series 1A: Radiographic Data	10-11
Fig. 6 Exposure Series 1B: Radiographic Data	13-14
Fig. 7 Exposure Series 2A: Radiographic Data	17-18
Fig. 8 Exposure Series 2B: Radiographic Data	19-20
Fig. 9 Exposure Series 3A: Radiographic Data	23-24
Fig. 10 Exposure Series 3B: Radiographic Data	26-27
Fig. 11 Exposure Series 4: Radiographic Data	30-31



## Abstract

The primary objective of this investigation was to determine the feasibility of detecting corrosion in aluminum Naval aircraft components with neutron radiographic interrogation and the use of standard corrosion penetrameters. Secondary objectives included the determination of the effect of object thickness on image quality, the defining of minimum levels of detectability and a preliminary investigation of a means whereby the degree of corrosion could be quantified with neutron radiographic data.

All objectives were met and may be summarized as follows: (1) Environment-induced corrosion can be detected with high sensitivity by thermal neutron radiographic interrogation, (2) the fluence at the image plane required to visualize corrosion with conventional imaging methods e.g., a gadolinium converter in conjunction with a medium contrast industrial x-ray film at density of 2.5, is approximately  $4 \times 10^8 \text{ n-cm}^{-2}$ . Assuming that a transportable neutron radiography system were capable of producing a flux of  $1.5 \times 10^4 \text{ n-cm}^{-2}\text{-sec}^{-1}$  at an L/D ratio of 40:1, an exposure of 7.4 hours would be required, (3) at an L/D ratio of 40:1, the corrosion signatures of both surfaces of a thick object, e.g., a wing or airfoil, must be interrogated individually. This is due to the fact that geometrical unsharpness obliterates signature detail on the surface opposite the cassette. (4) The possibility of corrosion quantification does exist. This conclusion is based on an investigation with standard corrosion plaque penetrameters, and (5) although the use of  $^{6}\text{LiF/ZnS}$  light emitting converters is the most efficient method by which thermal neutron beams can be imaged, the results are inadequate for unambiguous signature analysis with presently available converters.



## 1.0 Objectives

The primary objective of these investigations was to determine the feasibility of detecting corrosion in aluminum Naval aircraft components with neutron radiographic interrogation and the use of standard corrosion penetrameters. Secondary objectives included the determination of the effect of object thickness on corrosion image quality, the defining of minimum levels of detectability and a preliminary investigation of a means whereby the degree of corrosion could be quantified with neutron radiographic data.

## 2.0 Background

The nondestructive detection and visualization of environment-induced corrosion in aircraft presents an important maintenance problem and economic impact in both the civilian and military sectors. Since there is no reliable instrumental method by which corrosion can be detected in inaccessible areas of aircraft structures, visual and destructive inspection methods must presently be employed.

Corrosion in aircraft generally is induced by the presence of moisture and oxygen. The corrosion products so generated oftentimes, but not always, contain hydrogen in the forms of hydrated oxides or hydroxides. In the case of salt-water induced corrosion, chlorine may also be present. Because of the high attenuation of thermal neutrons by hydrogen and chlorine, it should be possible to visualize corrosion areas using neutron radiographic interrogation.

The basic procedures governing the neutron radiographic inspection methods employed in these studies are outlined in this report. In addition, the results of preliminary experiments at the National Bureau



of Standards to establish minimum levels of corrosion detectability and proposed methods to quantify the degree of corrosion are presented.

### 3.0 Experimental Facilities at the National Bureau of Standards

The Thermal Neutron Radiography Facility (TNRF) at the NBS 10MW Research Reactor was employed for these investigations. At a power level of 10MW, the reactor provided a thermal neutron flux of  $10^7 \text{ n-cm}^{-2}$   $\text{-sec}^{-1}$  at the image plane for an L/D ratio of 40:1. The L/D ratio of the facility was variable from a minimum of 40:1 to a maximum of 500:1. The neutron beam is highly thermalized, having a gold-cadmium ratio of 500:1. During the course of these studies, the neutron beam shutter was manually operated. A schematic diagram of the facility is illustrated in Figure 1.

### 4.0 Experimental Procedures: General

All radiographic data generated in these investigations was obtained using direct neutron imaging methods. Manual film development was performed throughout with Eastman Kodak standard industrial radiography chemistry. A 7 in.-thick section cut from an uncorroded C-2 aircraft vertical fin was used as a standard object to be radiographed. The fin, which was obtained from the NAVAIR Rework Facility at North Island, San Diego, CA is illustrated in Figure 2.

Standard corrosion penetrameters were fabricated from aircraft-grade aluminum which had been corroded under controlled environments for predetermined periods of time. The penetrometer samples were obtained from the Naval Air Development Center, Warminster, PA. Two types of penetrameters were employed in these investigations.



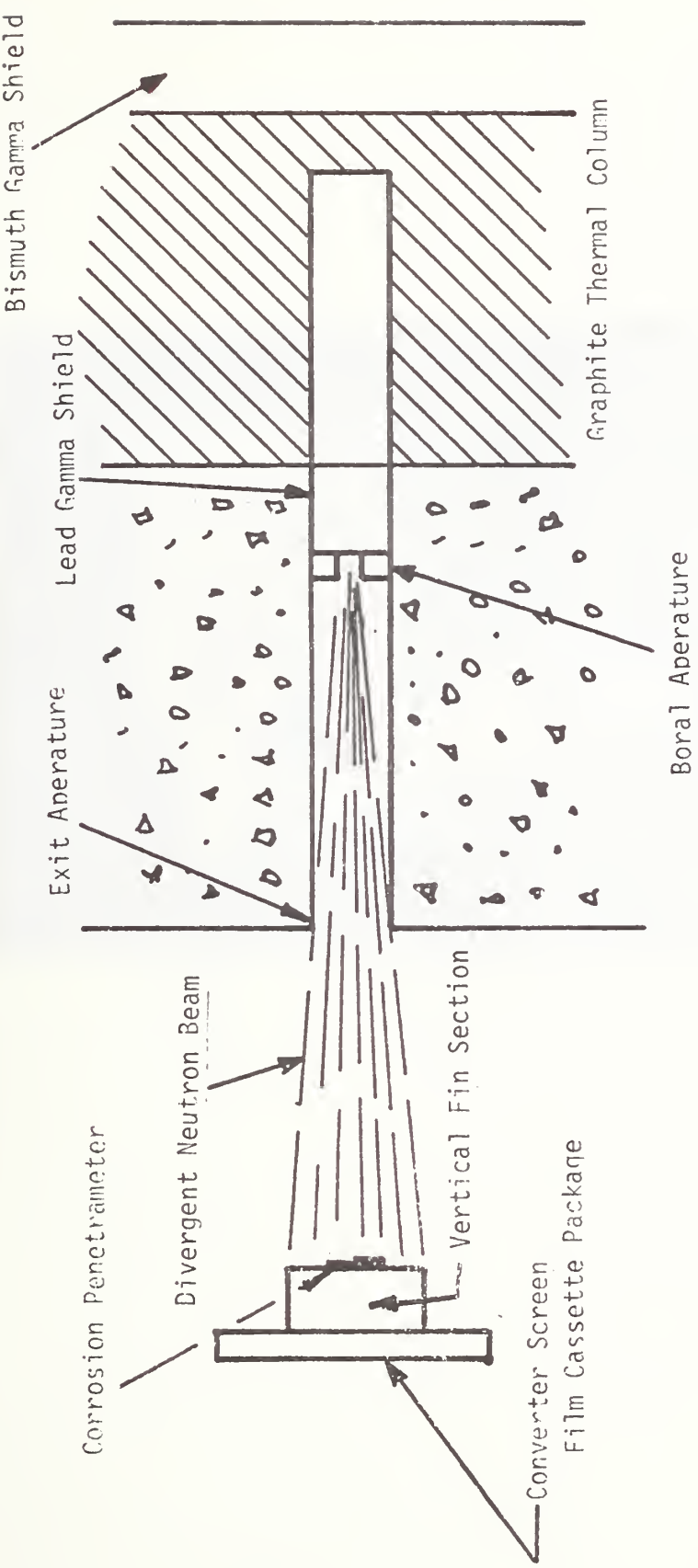


FIGURE 1. SCHEMATIC DIAGRAM OF THE NBS THERMAL NEUTRON RADIOPHOTOGRAPHY FACILITY



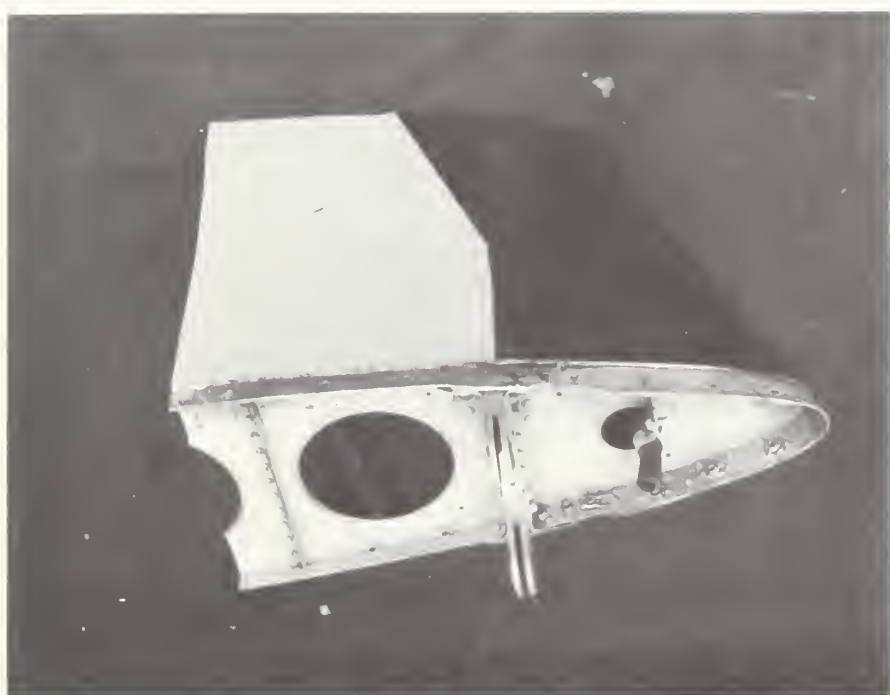


FIGURE 2. C-2 VERTICAL AIRFOIL



The first was fabricated from aircraft-grade aluminum which had been subjected to a super-saturated salt water spray for 6.5 hrs. Nominal step thicknesses were 0.125 in. and 0.87 in. Two views of this penetrameter are illustrated in Figures 3A and 3B. This penetrameter will be referred to as P-1 in this report.

The second set of four penetrameters was fabricated from 0.062 in.-thick aircraft-grade aluminum plates which had been subjected to a salt water spray/SO<sub>2</sub> gas environment for zero, four, eight and fifteen days. This set which will be referred to as P-2-1 through P-2-4 in this report, is illustrated in Figure 4. No effort was made to correlate the corrosion penetrameters with real life conditions. They were employed only to provide corrosion under standardized conditions.

## 5.0 Technical Approach

The tasks outlined in the program objectives were divided into four systematic experiments, each with one or more objectives. The objectives of each exposure series at the radiographic parameters employed, and the experimental results are illustrated.

## 6.0 Exposure Series 1 Through 3: General

The general objectives of this series of exposures were:

- (1) To determine the feasibility of utilizing neutron radiographic techniques to visualize corrosion areas in aircraft-grade aluminum employing several thermal neutron film-converter imaging techniques and a standard corrosion penetrameter.
- (2) To assess the effect of object thickness on the penetrameter image quality.
- (3) To observe the effect of analog edge enhancement on the penetrameter image quality.





FIGURE 3A. ALUMINUM CORROSION PENETRAMETER



FIGURE 3B. ALUMINUM CORROSION PENETRAMETER CLOSE-UP VIEW



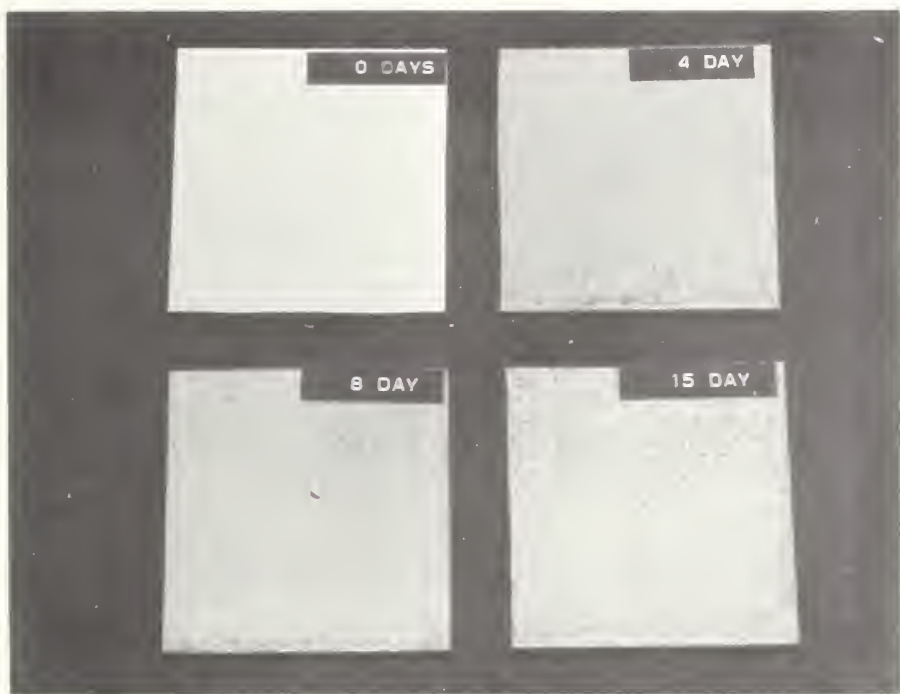


FIGURE 4. ALUMINUM CORROSION PENETRAMETERS P-2-1 THROUGH P-2-4



In exposure Series 1 through 3, the penetrrometer, object and geometry outlined below are identical, only the radiographic parameters are changed in each series. Radiographic exposures were made:

- (A) The penetrrometer P-1 alone.
- (B) The C-2 vertical fin section alone.
- (C) The C-2 vertical fin section with penetrrometer P-1 facing the cassette.
- (D) The C-2 vertical fin with the penetrrometer P-1 facing the collimated neutron source.
- (E) Analog edge enhanced image of C above.
- (F) Analog edge enhanced image of D above.

#### 6.1-A Exposure Series 1A

The radiographic parameters employed in the Exposure Series 1A are outlined in Table 1A below. This series of exposures serves to illustrate the radiographic data obtained utilizing a reactor-based system having a high (200:1) L/D ratio and employing medium-contrast (Kodak Type M) film. The radiographic data are illustrated in Figures 5A through 5F.

Table 1A: Exposure Series 1A: Radiographic Parameters

Converter	0.0005 in. Vapor Deposited Gd
Film Type	Kodak Type M
L/D Ratio	200:1
Exposure Time/Fluence	50 min./6 x 10 <sup>8</sup> n-cm <sup>-2</sup>
Neutron Beam Cd Ratio	500:1
Penetrometer	P-1
Object	C-2 Vertical Fin Section



Fig. 5: Exposure Series 1A: Radiographic Data



PENETRAMETER  
(A)



C-2 VERTICAL FIN  
(B)



C-2 VERTICAL FIN  
PENETRAMETER FACING CASSETTE  
(C)



C-2 VERTICAL FIN  
PENETRAMETER FACING SOURCE  
(D)



Fig. 5: Continued



ANALOG EDGE ENHANCEMENT PENETRAMETER  
FACING CASSETTE

(E)



ANALOG EDGE ENHANCEMENT PENETRAMETER  
FACING SOURCE

(F)



## 6.1-B Exposure Series 1B

The objective of this series of exposures was to determine the effect on the penetrrometer image quality when the L/D ratio was reduced from 200:1 to 43:1. These experiments provided comparative data of the results obtainable with a reactor-based system having a high L/D ratio to a source-based system having a low L/D ratio.

Radiographic parameters employed in Exposure Series 1B are outlined in Table 1B below.

Table 1B: Exposure Series 1B: Radiographic Parameters

Converter	0.0005 in. Vapor Deposited Gd
Film Type	Kodak Type M
L/D Ratio	43:1
Exposure Time/Fluence	90 sec./4 $\times 10^8$ n-cm <sup>-2</sup> (1)
Neutron Beam Cd Ratio	500:1
Penetrrometer	P-1
Object	C-2 Vertical Fin Section

The radiographic data derived from Exposure Series 1B are illustrated in Figures 6A through 6F.

### (1) Significant Parameter Change

## 6.1-C Exposure Series 1: Results and Conclusions

- (a) Salt water induced corrosion signatures in aircraft-grade aluminum can be visualized with neutron radiography using a 200:1 L/D ratio. The effect of the 7 in.-thick fin thickness is to degrade the image quality. However, the signature can still be discerned as illustrated in Figures 5C and 5D.



Fig. 6: Exposure Series 1B: Radiographic Data



PENETRAMETER

(A)



C-2 VERTICAL FIN

(B)



C-2 VERTICAL FIN  
PENETRAMETER FACING CASSETTE

(C)

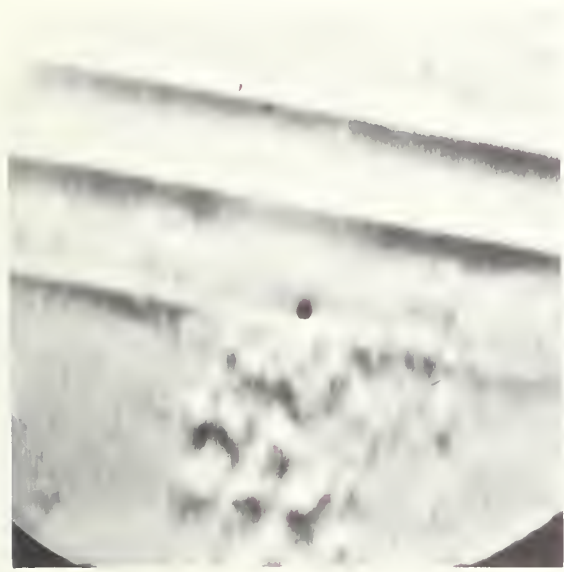


C-2 VERTICAL FIN  
PENETRAMETER FACING SOURCE

(D)



Fig. 6: Continued



ANALOG EDGE ENHANCEMENT PENETRAMETER  
FACING CASSETTE

(E)



ANALOG EDGE ENHANCEMENT PENETRAMETER  
FACING SOURCE

(F)



- (b) The time required for the exposure was 50 min. for a L/D ratio of 200:1.
- (c) With the penetrameter on either side of the fin, analog edge enhancement aids in identifying the corrosion signature.
- (d) When the L/D ratio is reduced to that of a field system, e.g., 43:1, The corrosion signature can only be visualized when the penetrameter was placed on the cassette side of the fin as shown in Figures 6C and 6D, making it necessary to inspect each side of an airfoil of 7 in. thickness individually.
- (e) The time required for the exposure was 90 sec. for a L/D ratio of 43:1.
- (f) With a L/D ratio of 43:1, image edge enhancement aids in visualizing the corrosion penetrameter when placed on the source side of the film, however, paint could possibly produce a similar signature.

#### 6.2-A Exposure Series 2A

In the group 2 series of exposures the 0.0005 in.-thick Gd converter has been replaced by a  $\text{Gd}_2\text{O}_2\text{S}$  converter. The radiographic parameters employed in this series of exposures is given in Table 2A below.



Table 2A: Exposure Series 2A: Radiographic Parameters

Converter	$\text{Gd}_2\text{O}_2\text{S}$	(2)
Film Type	Kodak Type M	
L/D Ratio	200:1	
Exposure Time/Fluence	$15 \text{ min.}/2 \times 10^8 \text{ n-cm}^{-2}$	(2)
Neutron Beam Cd Ratio	500:1	
Penetrometer	P-1	
Object	C-2 Vertical Fin	

The radiographic data resulting from exposure series 2A are illustrated in Figures 7A through 7F.

### (2) Significant Parameter Change

#### 6.2-B Exposure Series 2B

The objective of Exposure 2B was to examine the radiographic penetrometer P-1 using a  $\text{Gd}_2\text{O}_2\text{S}$  converter, when the L/D ratio was reduced from 200:1 to 43:1. The radiographic parameters employed in this exposure series are outlined in Table 2B below.

Table 2B: Exposure Series 2B: Radiographic Parameters

Converter	$\text{Gd}_2\text{O}_2\text{S}$	
Film Type	Kodak Type M	
L/D Ratio	43:1	(3)
Exposure Time/Fluence	$45 \text{ sec.}/2 \times 10^8 \text{ n-cm}^{-2}$	(3)
Neutron Beam Cd Ratio	500:1	
Penetrometer	P-1	
Object	C-2 Vertical Fin Section	

The radiographic data from this exposure series are illustrated in Figures 8A through 8F.

### (3) Significant Parameter Changes



Fig. 7: Exposure Series 2A: Radiographic Data



PENETRAMETER

(A)



C-2 VERTICAL FIN

(B)



C-2 VERTICAL FIN  
PENETRAMETER FACING CASSETTE

(C)



C-2 VERTICAL FIN  
PENETRAMETER FACING SOURCE

(D)



Fig. 7: Continued



ANALOG EDGE ENHANCEMENT PENETRAMETER  
FACING CASSETTE

(E)



ANALOG EDGE ENHANCEMENT PENETRAMETER  
FACING SOURCE

(F)



Fig. 8: Exposure Series 2B: Radiographic Data



PENETRAMETER

(A)



C-2 VERTICAL FIN

(B)



C-2 VERTICAL FIN  
PENETRAMETER FACING CASSETTE

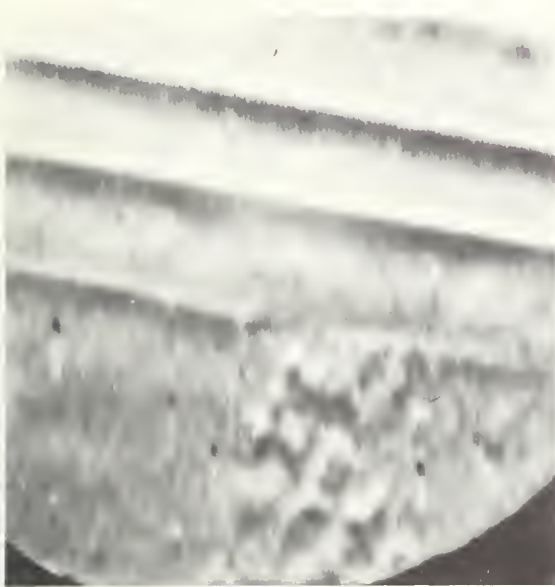
(C)

C-2 VERTICAL FIN  
PENETRAMETER FACING SOURCE

(D)



Fig. 8: Continued



ANALOG EDGE ENHANCEMENT PENETRAMETER  
FACING CASSETTE

(E)



ANALOG EDGE ENHANCEMENT PENETRAMETER  
FACING SOURCE

(F)



#### 6.2-C Exposure Series 2: Results and Conclusions

- (a) Corrosion signatures can be visualized using  $Gd_2O_2S$  converters with the penetrrometer placed on either side of the 7 in.-thick fin, using an L/D ratio of 200:1. The apparent contrast was not as high as that obtained with Gd foil, as illustrated in Figures 7C and 7D.
- (b) The exposure time required using a  $Gd_2O_2S$  converter was 15 min. for a L/D ratio of 200:1.
- (c) Image edge enhancement aided in identifying the corrosion signature on either side of the fin with a L/D ratio of 200:1.
- (d) When the L/D ratio was reduced to 43:1 using a  $Gd_2O_2S$  converter, the corrosion signature could only be visualized with the penetrrometer placed between the cassette and the fin as illustrated in Figure 8C. All image detail was eliminated due to geometrical unsharpness when the corrosion penetrrometer was placed on the source side of the fin as shown in Figure 8D.
- (e) The exposure required 45 sec. to complete.
- (f) Edge enhancement did aid in the visualization of the penetrrometer when it was placed between the fin and cassette, however, played little role in the detection of the corrosion signature when the penetrrometer was placed on the source side of the cassette.

#### 6.3-A Exposure Series 3A

The principal objectives of this exposure series was to determine the effect on penetrrometer P-1 image quality when the  $Gd_2O_2S$  converter



and Kodak Type M film were replaced by a  $^{6}\text{LiF/Zns}$  converter and light-sensitive Kodak Type Blue Brand film. The radiographic parameters of interest in this series of exposures is given in Table 3A below.

Table 3A: Exposure Series 3A: Radiographic Parameters

Converter	$^{6}\text{LiF/Zns}$ (4)
Film Type	Kodak Blue Brand (4)
L/D Ratio	200:1
Exposure Time/Fluence	5 sec./ $1 \times 10^6 \text{ n-cm}^{-2}$
Neutron Beam Cd Ratio	500:1
Penetrometer	P-1
Object	C-2 Vertical Fin Section

Radiographic data from Exposure 3A are illustrated in Figure 9A through 9F.

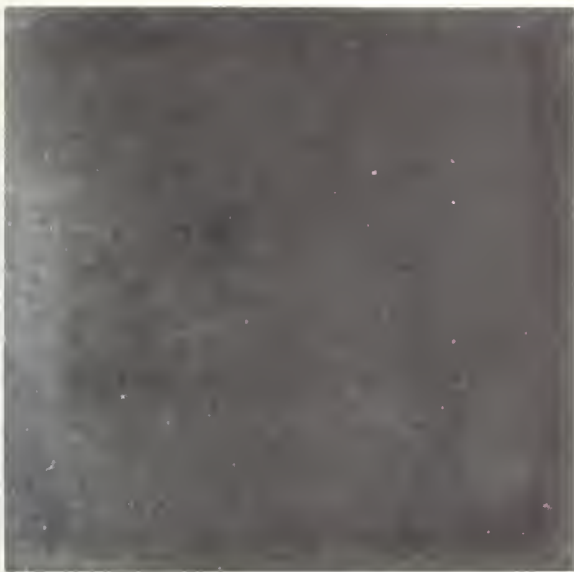
#### (4) Significant Parameter Change

#### 6.3-B Exposure Series 3B

This series of exposure was made to observe the effect of reducing the system L/D ratio from 200:1 to 43:1 on the image quality of the P-1 penetrometer. The  $^{6}\text{LiF/Zns}$  in combination with Kodak Blue Brand film imaging method remained the same as in Series 3A. The radiographic parameters employed in these series are presented in Table 3B below.



Fig. 9: Exposure Series 3A: Radiographic Data



PENETRAMETER

(A)



C-2 VERTICAL FIN

(B)



C-2 VERTICAL FIN  
PENETRAMETER FACING CASSETTE

(C)



C-2 VERTICAL FIN  
PENETRAMETER FACING SOURCE

(D)



Fig. 9: Continued



ANALOG EDGE ENHANCEMENT PENETRAMETER  
FACING CASSETTE

(E)



ANALOG EDGE ENHANCEMENT PENETRAMETER  
FACING SOURCE

(F)



Table 3B: Exposure Series 3B: Radiographic Parameters

Converter	$^6\text{LiF/Zns}$
Film Type	Kodak Blue Brand
L/D Ratio	43:1 (5)
Exposure Time/Fluence	0.2 sec./ $1 \times 10^6 \text{ n-cm}^{-2}$ (5)
Neutron Beam Cd Ratio	500:1
Penetrometer	P-1
Object	C-2 Vertical Fin Section

The radiographic data derived from these exposures is illustrated in Figures 10A through 10F.

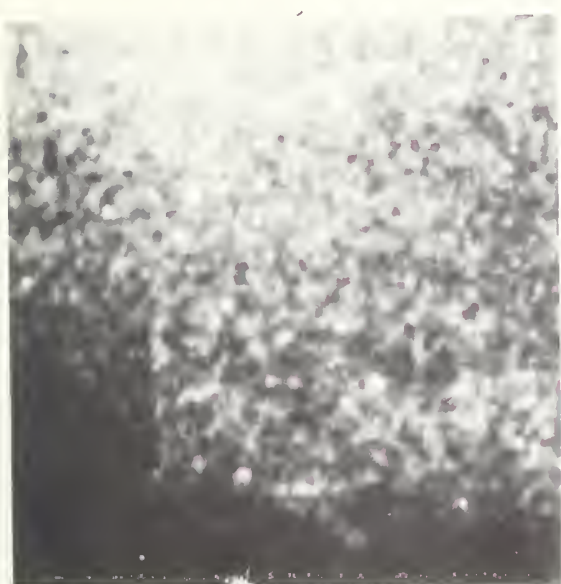
(5) Significant Parameter Change

6.3-C Exposure Series 3: Results and Conclusions

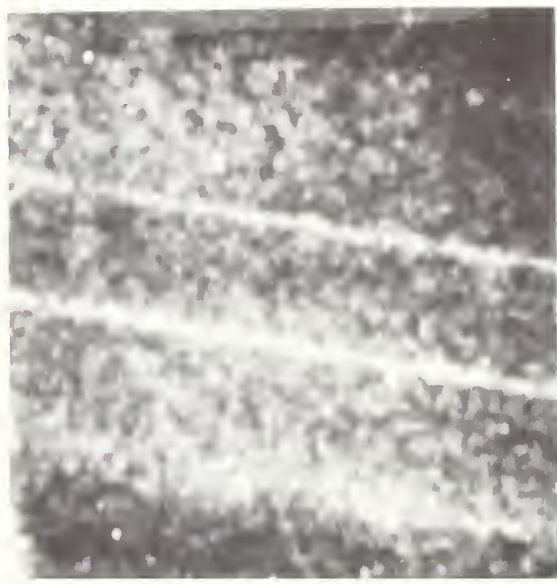
- (a) Using a Nuclear Enterprise NE 421  $^6\text{LiF/Zns}$  light-emitting converter in conjunction with Kodak Blue Brand film and a L/D ratio of 200:1, it was possible to visualize the corrosion signature when the penetrometer was placed between the vertical fin and cassette. The image quality was so poor however, that it could easily be confused with the scintillator mottling as illustrated in Figure 9C.
- (b) The exposure time required was 5 sec.
- (c) When the corrosion penetrometer was placed on the source side of the fin section, it was impossible to differentiate accurately between the corrosion signature and the background mottling.
- (d) Edge image enhancement provided no useful purpose in the visualization of the corrosion signature with the penetrometer on either side of the film.



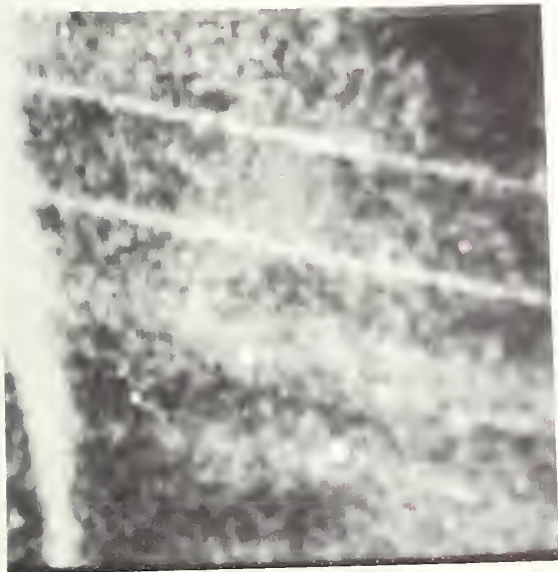
Fig. 10: Exposure Series 3B: Radiographic Data



PENETRAMETER  
(A)



C-2 VERTICAL FIN  
(B)



C-2 VERTICAL FIN  
PENETRAMETER FACING CASSETTE  
(C)



C-2 VERTICAL FIN  
PENETRAMETER FACING SOURCE  
(D)

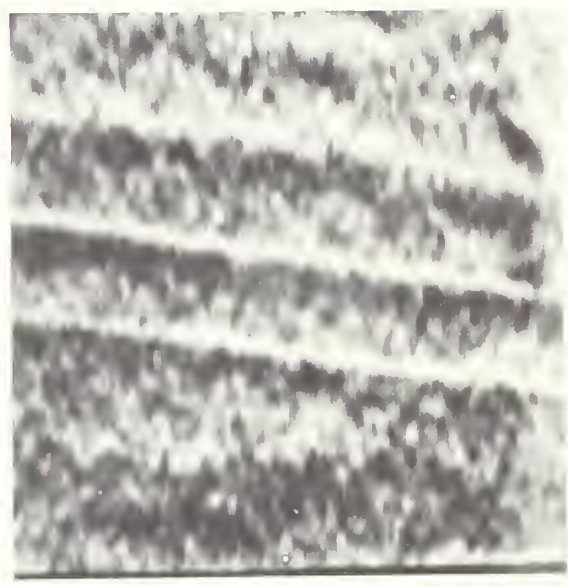


Fig. 10: Continued



ANALOG EDGE ENHANCEMENT PENETRAMETER  
FACING CASSETTE

(E)



ANALOG EDGE ENHANCEMENT PENETRAMETER  
FACING SOURCE

(F)



- (e) When the L/D ratio was reduced to 43:1, it was impossible to accurately distinguish between the corrosion signature and the background mottling with the penetrometer on either side of the vertical fin.
- (f) The exposure time required for this radiograph was approximately 0.2 sec.

#### 6.4-A Exposure Series 4: General

These investigations were conducted in an attempt to define the lower limit of corrosion detectability in aircraft-grade aluminum utilizing reactor-based neutron radiographic procedures. A set of four calibrated corrosion penetrometers P-2 were fabricated from 0.062 in.-thick aluminum plates which had been subjected to a salt water spray/SO<sub>2</sub> gas environment for 0, 4, 8 and 15 days. These penetrometers are illustrated in Figure 4. Thermal neutron radiographs were made of the seven inch thick C-2 vertical fin with calibrated penetrometers placed on the cassette side of the C-2 vertical fin.

The radiographic parameters employed for this set of exposures are given in Table 4 below.

Table 4: Exposure Series 4: Radiographic Parameters

Converter	0.0005 in.-Thick Vapor Deposited Gd
Film Type	Kodak Type M
L/D Ratio	100:1
Exposure Time/Fluence	30 min./18 x 10 <sup>8</sup> n-cm <sup>-2</sup>
Neutron Beam Cd Ratio	500:1
Object	C-2 Vertical Fin
Penetrometers	P-2-1 through P-2-4

The penetrometer calibrations are outlined in Table 5 below.



Table 5: Penetrometer Calibration

Penetrometer Number	Exposure Period to Salt Water Spray/SO <sub>2</sub> Gas Environment (Days)
P-2-1	0
P-2-2	4
P-2-3	8
P-2-4	15

The radiographic data illustrated in Figures 11A, 11C, 11E and 11G are video reproductions of penetrometers subjected to the corrosive environment for periods of 0, 4, 8 and 15 days respectively. The data illustrated in Figures 11B, 11D, 11E and 11G illustrate the edge enhanced reproductions respectively of these radiographs. It should be noted that the artifacts which appear as white dots in the neutron radiographic images were the result of dirt or other foreign neutron absorbing matter on the inside of the airfoil and were not images of the corrosion penetrometer.

#### 6.4-B Exposure Series 4: Results and Conclusions

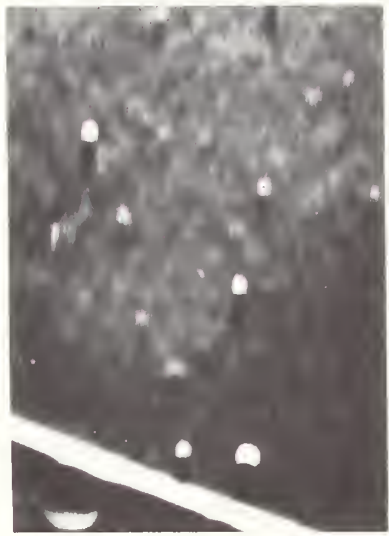
- (a) Thermal neutron radiographs of the four calibrated corrosion penetrometers P-2-1 through P-2-4 are illustrated in Figures 11A, 11B, 11C and 11D. These penetrometers were corroded with a salt water spray/SO<sub>2</sub> gas mixture for periods of 0, 4, 8 and 15 days respectively.
- (b) In the corrosion radiographs illustrated in Figures 11A and 11C, the corrosion cannot be distinguished from the background noise as shown in the edge enhanced illustrations in



Fig. 11: Exposure Series: Radiographic Data



(A)



(B)



(C)



(D)



Fig. 11: Continued



(E)



(F)



(G)



(H)



Figures 11E and 11F. It is likely that the mottled background noise is due to the neutron response to the fin paint.

- (c) Environment induced corrosion can be observed without image enhancement in the 8 and 15 day samples illustrated in Figures 11C and 11D respectively. Image enhancement serves to render the corrosion images more observable as illustrated in Figures 11G and 11H.

## 7.0 Quantification of Corrosion

Based on the experience gained in these preliminary investigations, empirical quantification of corrosion appears to be a possibility, either by isodensity scanning of neutron radiographs and comparison of scans of the corrosion areas with sound aluminum, or by digital image enhancement techniques. This conclusion is based on the fact that differences in corrosion density in the P-1 penetrameter could be visualized and that a minimum level of detectability could be established with the plaque penetrameters P-2-1 through P-2-4. Penetrometer P-1 was more easily seen than the P-2 series because of the greater degree of induced corrosion.

## 8.0 Remarks and Qualifications

It should be noted that the approach taken in these investigations was a very practical one in that the radiographic data obtained using ideal laboratory conditions was taken as a base, e.g., relatively high resolution imaging methods were employed. Comparative radiographic data were then obtained by varying the radiographic parameters to simulate a low-resolution system as might be the case in a transportable field unit neutron radiography system.



In the preparation of this report the conclusions reached were derived from actual radiographic data and not from photographic reproductions.

Photographic reproduction of high density radiographs was very difficult to accomplish for this report, e.g., the overexposure of Figure 5 compared to Figure 6 is not real, but is due to the photographic reproduction.

The data obtained in this work was limited to the use of film-converter imaging systems. No attempt was made to evaluate scintillator-coupled real time imaging systems.

#### 9.0 Summary

The significant results obtained from these investigations at the National Bureau of Standards may be summarized conclusively in the following statements.

- (1) Environment-induced corrosion in aircraft-grade aluminum can be detected with a high degree of sensitivity with thermal neutron radiographic interrogation.
- (2) The fluence (integrated neutron flux) at the image plane required to visualize corrosion with conventional imaging methods e.g., gadolinium converter in conjunction with a medium contrast industrial x-ray film at density of 2.5, is approximately  $4 \times 10^8 \text{ n-cm}^{-2}$ . Assuming that a transportable neutron radiography system were capable of producing  $1.5 \times 10^4 \text{ n-cm}^{-2\text{-sec}^{-1}}$  at a L/D ratio of 40:1, an exposure of 7.2 hrs would be required.
- (3) At a L/D ratio of 40:1, the corrosion signature of both surfaces of a thick object, e.g., a wing or airfoil, must be



interrogated individually. This is due to the fact that geometrical unsharpness obliterates signature detail on the surface opposite the cassette.

- (4) The possibility of corrosion quantification does exist, based on investigation with standard corrosion plaque penetrameters.
- (5) Although the use of  $^{6}\text{LiF}/\text{ZnS}$  light emitting converters is the most efficient method by which thermal neutron beams can be imaged, the results are inadequate for unambiguous corrosion signature analysis using presently available converters. The reasons for this are described below.

## 10.0 Recommendations for Future Work at NBS

### 10.1 Converter Development

The most efficient light-emitting neutron imaging system in so far as speed is concerned consists of a physical mixture of  $^{6}\text{LiF}$  and ZnS powders. The components are held in suspension with a binder and settled on a thin aluminum substrate. The nuclear reaction which takes place is  $^{6}\text{Li}(\text{n},\text{T})\alpha$ , the tritons and alpha particles producing light in the ZnS scintillator.

The neutron radiographic images produced when this type of imaging screen is placed in intimate contact with light-sensitive film is quite grainy, exhibiting poor resolution. This is due, in fact, to several factors which include:

- (a) The fact that the matrix is composed of powders having a finite grain size. If this grain is too coarse, a granular image will result.



- (b) The  $^{6}\text{LiF}/\text{ZnS}$  is partially transparent to light generated within the matrix, making it possible for light generated at one point to be scattered and emitted at a neighboring site.
- (c) Light sensitive films generally tend to exhibit greater grain than industrial x-ray films.

We propose that a funded R & D program be initiated at NBS to develop a neutron-sensitive scintillating converter which will overcome the aforementioned problems of the presently available continuous  $^{6}\text{LiF}/\text{ZnS}$  thermal neutron imaging screens. Specifically, (1) we propose to size the  $^{6}\text{LiF}/\text{ZnS}$  components so that only the finest grains available are employed to mix the final matrix using a fluorocarbon binder and (2) to break the initial continuous screen into a myriad of discrete information centers, or cells in order to eliminate the cross-talk generated as a result of the light transmission within the scintillator screen matrix. We have in mind to deposit the converter matrix in individual cells using chemically milled meshes having cells of approximately 0.001 in. on a side separated by 0.005 in. walls to minimize cross-talk.

#### 10.2 Real-Time Imaging Methods for Corrosion Detection

Pending the outcome of the screen-development work, we propose that an evaluation of state-of-the-art real-time imaging systems be conducted for corrosion detection under field conditions. It would be most cost effective to evaluate the available real-time imaging systems on a lease basis.

This method has the advantage of speed based on the assumption that a suitable fast imaging screen can be developed which would provide the required resolution.



### 10.3 Corrosion Quantification Standard Penetrometer Development

The quantification of detectable corrosion could produce an economic impact on military aircraft maintenance costs based on the assumption that short exposure times can be achieved. By being able to quantify the corrosion, it should be possible to predict the time at which a defective area of skin or component should be replaced, rather than replacement on a preventative maintenance basis. This is contingent on the fact that a fast, high resolution imaging screen can be developed which would result in reasonable exposure times.

We propose that several avenues of investigations towards this end be pursued, e.g.

- (1) Automated radiographic image analysis based on the isodensity pattern comparison with standard corrosion penetrometers or edge enhanced shadow analysis.
- (2) Microchemistry of actual aircraft corrosion samples to aid in the fabrication of standard corrosion penetrometers for use as Standard Reference Materials.
- (3) Subtraction of x-ray data from neutron data to eliminate the radiographic interferences caused by structural airframe thickness variation.



## EDITORIAL RECORD (Manuscript Approval Form)

STRUCTIONS: Attach original and 2 copies (photocopies) of this form to manuscript and send to: The Secretary, appropriate Editorial Review Board. Complete form as indicated below.

Div. and Sec.	Cost Center No. (Div. use only)	Signature of Section Chief	Date
314.00		<i>Reverend</i>	12-22-77
Signature: Division Editorial Committee Chairman	Date	Signature of Division Chief	Date
		<i>Reverend</i>	12-22-77
Signature of readers for division	Date	Total manuscript pages (including tables)	
<i>Harvey Alpern</i>	1/12/78	Is material in automated form? If so, supply 2 copies of ms.	
		Number of drawings	
		Number of photos	

## TITLE OF PAPER:

THE MACROSCOPIC DETECTION OF CORROSION IN ALUMINUM AIRCRAFT STRUCTURES WITH THERMAL NEUTRON BEAMS AND FILM IMAGING METHODS

AUTHOR(S) (TYPED) Include Title and Telephone Extension	Author(s) Signature and date	AFFILIATION (If NBS give Division and Section)
Donald A. Garrett X3634		314.00

## To: Institute Director

From: Division Chief \_\_\_\_\_  
(Initials)

- Paper requires specific review and approval (Chap. 4.2 NBS Manual)  
 Paper requires approval for publication in foreign medium

Approved \_\_\_\_\_  
Institute Director (Signature) \_\_\_\_\_ Date \_\_\_\_\_

## To: Editorial Review Board

From: *Reverend* 12-22-77  
Division Chief (Signature) \_\_\_\_\_ Date \_\_\_\_\_

- Paper requires policy review only  
 Paper requires technical and policy review

Patent review is:  in progress;  requested;  not required.

## APPROVED BY NBS EDITORIAL REVIEW BOARD (WERB-BERB-JILA) IF APPLICABLE

## APPROVAL

Signatures of reviewers for Editorial Review Board	Date	Sponsor	Date

## BOARD MEMBERS

## J. RES. EDITOR APPROVAL

## RELEASED FOR PUBLICATION

	Date	Signature of authorized official and date
		NBS PUBLICATION NUMBER <i>77-1144</i>



U.S. DEPT. OF COMM. BIBLIOGRAPHIC DATA SHEET		1. PUBLICATION OR REPORT NO. <b>NBSIR 78-1434</b>	2. Gov't Accession No.	3. Recipient's Accession No.
TITLE AND SUBTITLE		THE MACROSCOPIC DETECTION OF CORROSION IN ALUMINUM AIRCRAFT STRUCTURES WITH THERMAL NEUTRON BEAMS AND FILM IMAGE METHODS		
AUTHOR(S)		5. Publication Date		
<b>Donald A. Garrett</b>		6. Performing Organization Code		
PERFORMING ORGANIZATION NAME AND ADDRESS		8. Performing Organ. Report No.		
NATIONAL BUREAU OF STANDARDS DEPARTMENT OF COMMERCE WASHINGTON, D.C. 20234		10. Project/Task/Work Unit No.		
Sponsoring Organization Name and Complete Address (Street, City, State, ZIP)		11. Contract/Grant No.		
		13. Type of Report & Period Covered		
SUPPLEMENTARY NOTES		14. Sponsoring Agency Code		

ABSTRACT (A 200-word or less factual summary of most significant information. If document includes a significant bibliography or literature survey, mention it here.)

The primary objective of this investigation was to determine the feasibility of detecting corrosion in aluminum Naval aircraft components with neutron radiographic interrogation and the use of standard corrosion penetrameters. Secondary objectives included the determination of the effect of object thickness on image quality, the defining minimum levels a detectability and a preliminary investigation of means whereby the degree of corrosion could be quantified with neutron radiographic data.

All objectives were met and may be summarized as follows: (1) Environment-induced corrosion can be detected with high sensitivity by thermal neutron radiographic interrogation, (2) the fluence at the image plane required to visualize corrosion with conventional imaging methods e.g., a gadolinium converter in conjunction with a medium contrast industrial x-ray film at density of 2.5, is approximately  $4 \times 10^8$  n-cm<sup>-2</sup>. Assuming that a transportable neutron radiography system were capable of producing a flux of  $1.5 \times 10^4$  cm<sup>-2</sup>-sec<sup>-1</sup> at an L/D ratio of 40:1, an exposure of 7.2 hours would be required, (3) at a L/D ratio of 40:1, the corrosion signatures of both surfaces of a thick object, e.g., wing or airfoil, must be interrogated individually. This is due to the fact that geometrical unsharpness obliterates signature detail on the surface opposite the cassette, (4) The possibility of corrosion quantification does exist. This conclusion is based on investigation with standard corrosion plaque penetrameters, and (5) although the use of <sup>6</sup>LiF/ZnS light emitting converters is the most efficient method by which thermal neutron beams can be imaged, the results are inadequate for unambiguous signature analysis with presently available converters.

KEY WORDS (six to twelve entries; alphabetical order; capitalize only the first letter of the first key word unless a proper name; separated by semicolons)

Aircraft corrosion; corrosion; corrosion characterization; corrosion detection; corrosion quantification; hidden corrosion detection with neutron beams; neutron radiography

AVAILABILITY	<input checked="" type="checkbox"/> Unlimited	19. SECURITY CLASS (THIS REPORT)	21. NO. OF PAGES
<input type="checkbox"/> For Official Distribution. Do Not Release to NTIS		UNCLASSIFIED	
<input type="checkbox"/> Order From Sup. of Doc., U.S. Government Printing Office Washington, D.C. 20402, SD Cat. No. C13		20. SECURITY CLASS (THIS PAGE)	22. Price
<input checked="" type="checkbox"/> Order From National Technical Information Service (NTIS) Springfield, Virginia 22151		UNCLASSIFIED	

